

Article

Thermal Performance of Residential Roofs in Malaysia: Experimental Study Using an Indoor Solar Simulator

Muhamad Zahin Mohd Ashhar and Chin Haw Lim * 

Solar Energy Research Institute, Universiti Kebangsaan Malaysia, Bangi 43600, Selangor, Malaysia; zahinashhar@gmail.com

* Correspondence: chinhaw.lim@ukm.edu.my

Abstract: Previous researchers have detailed the problems in measuring the thermal resistance value of a whole roof assembly under hot conditions due to the uncertainty of the outdoor environment. Currently, no established method exists to experimentally investigate an entire thermal roof performance under a steady-state condition. This article details the properties of the indoor solar simulator and the research methods undertaken to measure the thermal resistance value of roof assembly. The indoor solar simulator utilizes 40 halogen bulbs to accurately replicate sun radiation. Thermocouples and heat flux sensors are installed at several locations on the roof assembly to quantify the heat transmission occurring through it. The thermal resistance value is determined by adding up the average difference in temperature across the external and internal roof surfaces and dividing the total amount by the total of all averaged heat fluxes. Subsequently, this study investigates the thermal efficiency of residential roof assemblies that comprise various insulation materials frequently employed in Malaysia, including stone wool, mineral glass wool, reflective bubble foil insulation, and radiant barriers. The analysis showed that the roof configurations with bubble foil reflective insulation produce superior thermal resistance values when coupled with enclosed air space or mass insulation, with thermal resistance values ranging between 2.55 m²K/W and 3.22 m²K/W. It can be concluded that roof configurations with bubble foil reflective insulation resulted in high total thermal resistance and passed the minimum thermal resistance value of 2.5 m²K/W under the Malaysian Uniform Building By-Law 38 (A) requirements. Furthermore, the radiant barrier produced a high thermal resistance value of 2.50 m²K/W when installed parallel to a 50 mm enclosed air space, emphasising the crucial function of an enclosed air space next to a reflective foil to resist the incoming heat radiation. The findings from this research can help building professionals determine the optimum insulation for residential building roofs in Malaysia.

Keywords: radiant barrier; indoor solar simulator; mass insulation; thermal resistance; reflective insulation



Citation: Mohd Ashhar, M.Z.; Lim, C.H. Thermal Performance of Residential Roofs in Malaysia: Experimental Study Using an Indoor Solar Simulator. *Buildings* **2024**, *14*, 178. <https://doi.org/10.3390/buildings14010178>

Academic Editor: Jiying Liu

Received: 23 November 2023

Revised: 22 December 2023

Accepted: 8 January 2024

Published: 10 January 2024



Copyright: © 2024 by the authors. Licensee MDPI, Basel, Switzerland. This article is an open access article distributed under the terms and conditions of the Creative Commons Attribution (CC BY) license (<https://creativecommons.org/licenses/by/4.0/>).

1. Introduction

Malaysia experiences hot and humid conditions all year long. Buildings in Malaysia depend highly on air-conditioning to keep indoor environments cool and comfortable. As a result, commercial and residential buildings are responsible for 12% of Malaysia's total energy consumption [1]. Due to this problem, passive strategies have been introduced to lower building energy consumption and elevate indoor thermal comfort. Local building authorities have advised using roof insulation to reduce the heat intake into a building through the roof component. Malaysian local authority has introduced a new by-law 38A (2) of the Uniform Building By-Laws (UBBLs), which states that the roof of all non-residential and residential buildings must achieve a thermal transmittance (U-value) lower than 0.4 W/m²K or must achieve a thermal resistance (RSI value) higher than 2.5 m²K/W [2]. However, a precise method to experimentally evaluate a roof assembly's RSI value or U-value is yet to be established.

1.1. Research Background

The roof is one of the main components of a building envelope responsible for high heat gain. It is constantly exposed to solar radiation, especially for buildings with large and poorly insulated roof surfaces [3]. Poorly insulated roofs can contribute to a large amount of air conditioning usage. For example, a previous study showed that the solar radiation absorbed by a roof surface contributes to more than 40% of the top floor spaces' electrical energy during hot summer [4]. In tropical countries, building sectors consume roughly 57% of the nation's total electrical energy, and 60% of the electrical energy in the building sector is from air conditioning systems [5]. Past research proves that roof insulation is an effective passive cooling method to reduce heat intake through the roof and reduce building energy consumption [6].

Thermal insulation is a proven passive technique for lowering heat intake through the roof component. Typically, there are two main thermal insulation types: mass insulation (or bulk insulation) and reflective foil [7]. A reflective foil is generally an aluminium sheet with low emissivity ($\epsilon \leq 0.05$) and high reflectivity characteristics. It is proven to reflect 95–99% of radiative heat transfer. Reflective foil is divided into two categories: radiant barriers and reflective insulation. A radiant barrier is a single sheet of aluminium foil with a reflective surface.

In contrast, reflective insulation is aluminium foil attached to foam or air bubbles. Incorporating air bubbles and foam in reflective insulation traps air and thus minimises heat transfer via conduction and convection [8]. In a roof assembly, the low emissivity side of the radiant barrier or reflective insulation must be installed parallel to an enclosed air space to efficiently reflect the incoming heat transfer, as seen in Figure 1.

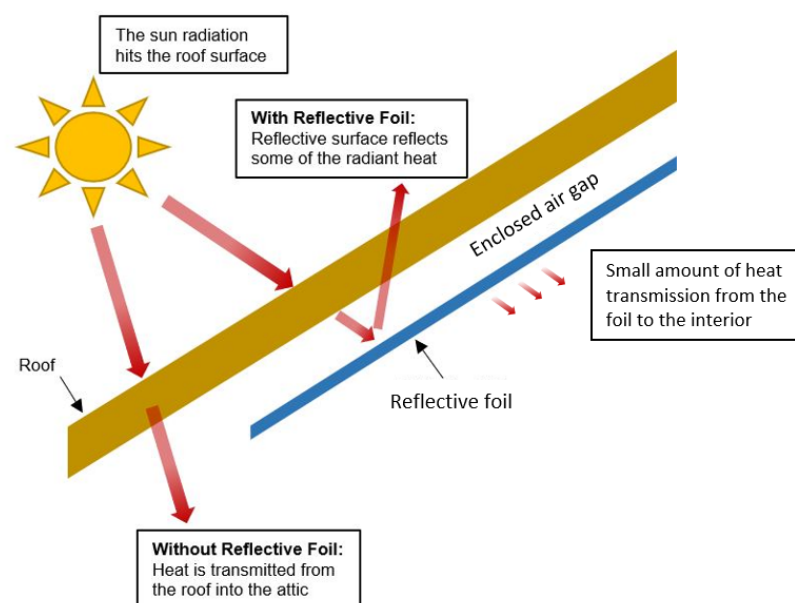


Figure 1. Illustration of how reflective foil works as a roof thermal insulation [9].

Mass insulation, such as mineral glass wool and stone wool, is another common insulation in Malaysian buildings. Both mineral glass wool and stone wool have similar manufacturing processes. The only difference is that mineral glass wool is manufactured from natural and recycled glass, whereas stone wool is made from basalt. Although both insulations claim to have similar thermal properties, stone wool products have better fire-resistant performance than mineral glass wool [10]. Mineral glass wool and stone wool have small, isolated, and trapped air pockets. The trapped air pockets prevent heat gain via convective heat transfer by preventing heat from transferring from one air pocket to the next. If the insulation is compressed, the air pockets will be extinguished, disrupting the

thermal performance [11]. Hence, in the building envelope, the mineral glass wool or stone wool must be installed with spacers to ensure that they are not compressed and that the thermal performance remains optimum.

1.2. Previous Work

In Malaysia, residential buildings such as landed houses commonly use roof tiles with attic space as the roof assembly. Concrete roof tiles are widely used as they are durable, cost-effective, and easy to maintain. Many studies in the literature have investigated the effectiveness of roof insulations.

Past literature has discussed the effectiveness of reflective foil with low emissivity as a roof insulation method in both summer and winter weather conditions. Shrestha et al. [12] studied an entire roof attic to study its performance in various climatic conditions in a large-scale climate simulator. Low emissivity reflective foil with various emissivity ($\epsilon = 0.02, 0.03, \text{ and } 0.23$) was used for the roof insulation. The study shows that the low emissivity reflective foil managed to lower the heat intake into the attic by 19.9% to 49.8% under summer conditions. In winter, the reflective foil decreased the thermal waste from the attic by 5.7% to 10.0%. Fantucci and Serra [13] compared the thermal performance of reflective paint and reflective insulation in a pitched roof of a residential building under construction in Italy. It was found that a reduction in indoor summer heat of between 10% and 53% can be achieved depending on the surface emissivity.

Similarly, Ferreira and Corvacho [14] used a detached house to compare the thermal performance of TRB, a radiant barrier attached below the truss/rafter, and HRB, a radiant barrier attached horizontally to the ceiling. Although HRB could perform well and reduce heat flux transmission by 70–73% during summer days, the TRB was considered a better option as it abolished the problem of dust accumulation on the radiant barrier. This is because dust accumulation on the HRB could reduce the emissivity, thus reducing the thermal performance of the radiant barrier. Michels et al. [15] used a pitched roof of a residential house in Brazil to examine the thermal efficiency of a radiant barrier under clay roof tiles assembly. The study showed that the radiant barrier managed to lower the heat flux transmission by up to 70% and reduced the ceiling temperature by 8 °C during the summer days. Teh et al. [16] compared the thermal performance of bubble and woven aluminium foil in two identical test cells with gable roofs. The heat flux transmission reduction for both reflective foils was roughly 80–90% compared to uninsulated roofs. Furthermore, the attic air temperature reduction increases when the air space thickness between the roof tiles and the reflective foil is thicker.

Previous research detailed the thermal roof performance of roofs insulated with mass insulation and reflective foil. For example, Medina [17] studied the effectiveness of combining several ceiling mass insulation levels with radiant barriers using computer simulation. The simulation results revealed that the radiant barrier's contribution in reducing the heat transfer through the ceiling dropped from 42% to 25% when the ceiling insulation increased from 1.94 m²K/W to 5.28 m²K/W. Therefore, the mass insulation level must be optimized to maximize the reflective insulation's effectiveness. D'Orazio et al. [18] compared the thermal performance of a pitched roof of a single-story building with and without reflective insulation. The study found that reflective insulation decreases heat flux transmission by 17% compared to the roof without reflective insulation.

Furthermore, the reflective insulation reduced 10% of heat loss during cold nights compared to uninsulated roofs. The researchers also detailed that combining high levels of mass insulation and reflective insulation will reduce the effectiveness of the reflective insulation. Hauser et al. [19] used two gable roofs in Germany to compare the thermal roof performance of reflective insulation and mineral wool. During the winter, the reflective insulation loses double the heat energy of mineral wool. This shows mineral wool saves more heating energy than reflective insulation during winter. Furthermore, the calculated R-value of the roof system with mineral wool was three times higher than that of reflective insulation. Amer [20] investigated the combination of 5 cm thick glass wool and aluminium

foil as the insulation method below the roof. The combination of glass wool and aluminium reduced the indoor air temperature by 2.6 °C compared to the ambient temperature. Ong [21] experimented with a 50 mm thick stone wool and a radiant barrier to insulate cement tiles on a small gable roof. It was found that the combination of the stone wool and radiant barrier was able to reduce the attic temperature to as low as 30 °C when the insulations are installed directly below the cement roof tiles. Muhieldeen et al. [22] examined the optimum thickness of glass wool as the roof insulation to reduce indoor air temperature and heat flux transmission. The results showed that the glass wool thickness of 25 mm, 50 mm, and 75 mm managed to lower the indoor air temperature by 1.0 °C, 1.3 °C, and 1.5 °C, and heat flux transmission by 3%, 12%, and 20%, respectively. Although the 75 mm thick glass wool reduced indoor air temperature and heat flux transmission, the 50 mm glass wool is the most optimum as it is the most cost-effective, with a return on investment of 27.40% per year.

Few previous research has attempted to calculate insulated roof systems' thermal resistance (RSI value). However, it is still very challenging for the researchers to determine the RSI value of a steady-state condition in summer via empirical measurement. This is due to the significant temperature fluctuations and unstable climate boundary conditions during summer days [19,23]. Therefore, this paper aims to evaluate the RSI value of thermally insulated roof assemblies using a novel indoor solar simulator.

1.3. Research Objectives

This study uses a novel indoor solar simulator to assess the thermal efficiency of thermally insulated roof assemblies for residential buildings. Furthermore, this research compares the effectiveness of several types of insulation commonly used for residential roofs in Malaysia, such as bubble foil reflective insulation, radiant barriers, mineral glass wool, and stone wool, using a novel indoor solar simulator in a steady-state laboratory environment.

2. Laboratory Measurement—Indoor Solar Simulator

The objective of the indoor solar simulator is to examine the thermal performance of roofs in a controlled indoor laboratory setting under steady-state conditions. The experimental measurement needs to occur in a steady-state condition so that the RSI value of the whole roof assembly can be calculated with high accuracy. There is minimal air movement inside the laboratory; thus, this study considers the wind effect negligible. The advantage of the indoor solar simulator is that any desired roof configuration can be assembled and assessed in a shorter period with high accuracy. As seen in Figure 2, 40 units of halogen lamps are fixed above the roof assembly to simulate solar radiation. Previously, the invention of the novel solar simulator was patented with the grant number MY-194877-A.

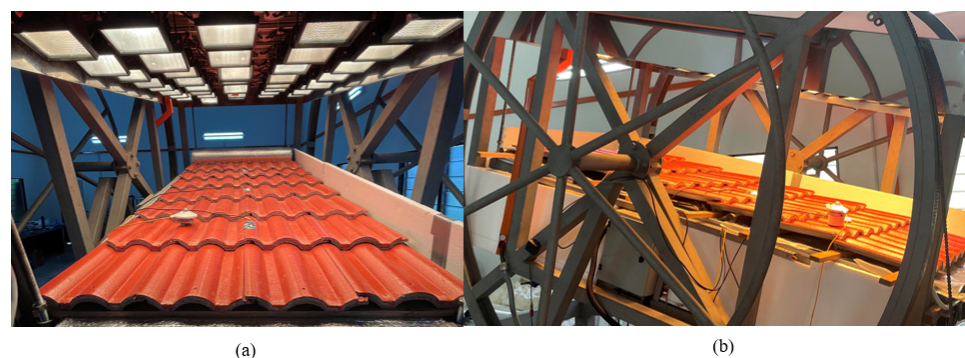


Figure 2. (a) A total of 40 halogen lamps simulating the solar radiation; (b) side view of the indoor solar simulator.

2.1. Sensors and Data Acquisition System

To measure the thermal response of the roof assembly, thermocouples, and heat flux sensors were placed at several locations of the roof assembly. The properties of the sensors are as detailed in Table 1. This research used K-type thermocouples to quantify the surface temperature of different roof surfaces. In addition, heat flux sensors (GHT-2C-ENV#0695) were used to quantify the heat flow transmission across different roof surfaces. Three units of thermocouples were placed on the upper surface of the roof tiles (T_{1A} , T_{1B} , and T_{1C}), three units of thermocouples were placed at reflective foil's lower surface (T_{2A} , T_{2B} , and T_{2C}), and three units of thermocouples were placed on the gypsum board (T_{3A} , T_{3B} , and T_{3C}). The purpose of having three thermocouples on the surfaces is to obtain the average surface temperature. Besides that, one heat flux sensor unit is positioned on the bottom surface of the reflective foil (q_1) and one heat flux sensor unit is located beneath the gypsum board (q_2). The sensors transmit signals every minute, and the Arduino controller and data acquisition system acquire the readings. The roof inclination angle is adjusted to 15° . The total roof size that can be assembled on the indoor solar simulator is 3 m in length and 1.5 m in width. Figure 3 shows the roof assembly setup and the sensor positions on the roof assembly.

Table 1. Sensors used for the measurement using the indoor solar simulator.

Equipment	Manufacturer	Function	Accuracy	Range	Reference
K-type thermocouple 	RS Components (London, UK)	To obtain the temperature of a surface	$\pm 1^\circ\text{C}$	$-200\text{--}1000^\circ\text{C}$	[24]
Heat Flux Sensor (GHT-2C-ENV#0695) 	International Thermal Instrument Company, Inc. (Del Mar, CA, USA)	To evaluate heat flux transmission across a surface	$\pm 1\%$	$0\text{--}3155\text{ W/m}^2$	[25]
Pyranometer 	Kipp & Zonen (Delft, The Netherlands)	Measure solar irradiance	$\pm 3\%$	$0\text{--}2000\text{ W/m}^2$	[26]

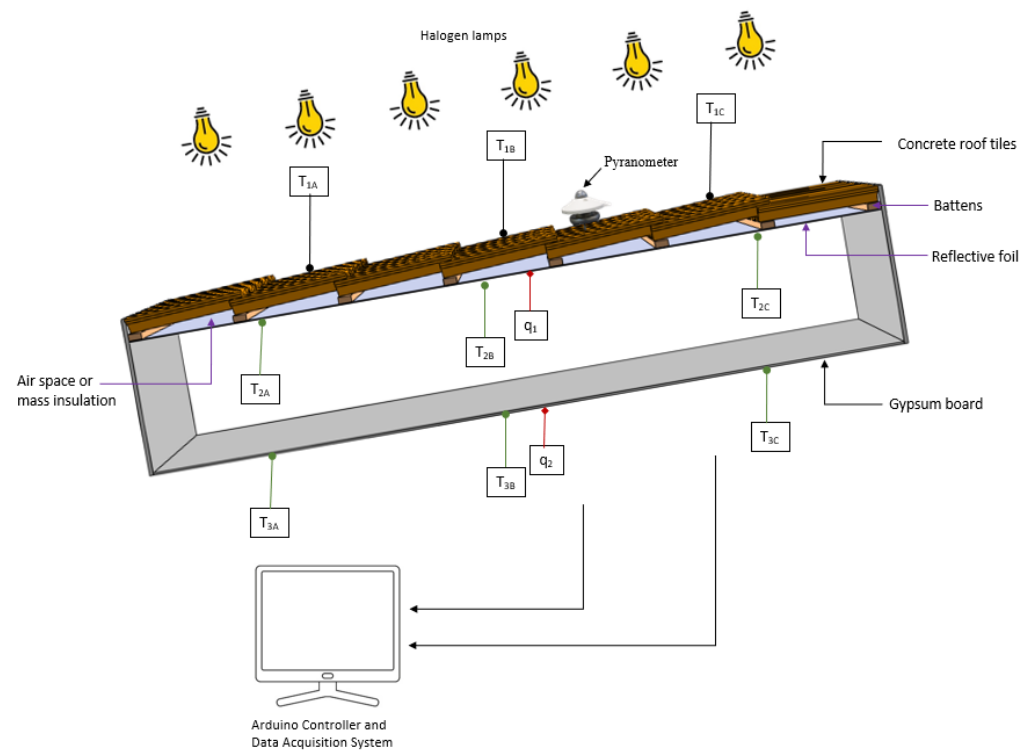


Figure 3. Schematic diagram showing the setup of the roof assembly and the location of the sensors on the roof assembly.

2.2. Properties of the Concrete Roof Tile and Insulation Materials

Concrete roof tiles are commonly used for residential buildings in Malaysia. Depending on the roof configuration, concrete roof tiles are usually insulated with thermal insulations such as mass insulation (mineral glass wool or stone wool) and reflective foil (radiant barrier and reflective insulation). The properties of concrete roof tiles and the insulation materials used in this research are detailed in Table 2.

Table 2. Specification of the concrete roof tile and insulation materials.

Material	Specification
 <p>Concrete roof tile</p>	<p>Extruded concrete roofing tile with fused pigmented colour coating [27]; Thickness: 12 mm; Thermal conductivity = 0.836 W/mK; RSI value = 0.014 m²K/W.</p>

Table 2. Cont.

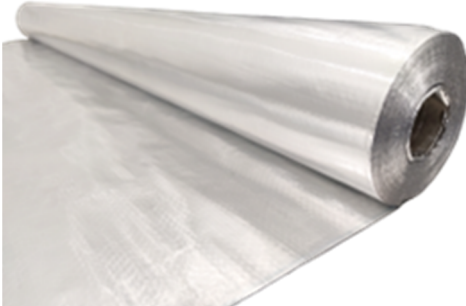
Material	Specification
	<p>Stone wool is made of basalt—a type of volcanic stone. It is non-combustible, which also can be used for thermal insulation, fire, and sound protection. At a thickness of 50 mm and a density of 40 kg/m^3, it has an RSI value of $1.39 \text{ m}^2\text{K/W}$ and thermal conductivity of 0.036 W/mK [28].</p>
Stone wool	
	<p>Mineral glass wool is commonly used as insulation for metal deck roofs and roof tiles. At a thickness of 50 mm and density of 16 kg/m^3, it has a thermal conductivity of 0.0366 W/mK and RSI value of $1.35 \text{ m}^2\text{K/W}$ [29].</p>
Mineral glass wool	
	<p>The radiant barrier is an aluminium foil laminated to a high-density polyurethane woven fabric. One side of the surface is pure aluminium with a low emissivity of 0.02. Another side of the surface is made out of metalized aluminium. The thickness of the radiant barrier is 0.17 mm and has a density of 160 g/m^2 [30]. It has an RSI value of $0.000 \text{ m}^2\text{K/W}$.</p>
Radiant barrier	
	<p>Bubble foil reflective insulation is aluminium laminated to a polyethylene bubble sheet. Both sides of the surfaces are made out of pure aluminium with a low emissivity value of 0.01. The bubble pockets have a diameter of 10 mm and a density of 380 g/m^2. The thermal conductivity is 0.0537 W/mK, and the RSI value of the material is $0.1694 \text{ m}^2\text{K/W}$. The thickness of the foil is 9 mm [31].</p>
Bubble foil reflective insulation	

Table 2. Cont.

Material	Specification
	<p>Gypsum plasterboard as the ceiling. It has a thickness of 12 mm. Density: 9.7 kg/m²; Thermal conductivity: 0.25 W/mK; RSI value: 0.05 m²K/W.</p>
Gypsum ceiling board	

3. Methodology

3.1. Test Method Validation Using Outdoor Roof Tile Surface Temperature

The concrete roof tiles' outdoor surface temperature value was used to justify the test method undertaken using the indoor solar simulator. Figure 4 displays the measurement of the surface temperature of roof tiles on a typical hot and clear bright day in Malaysia. The average temperature recorded on that particular day was 30 °C, while the highest temperature was 33 °C. Obtaining the steady-state figure of heat flux transmission was challenging due to the dynamic nature of the outside environment.

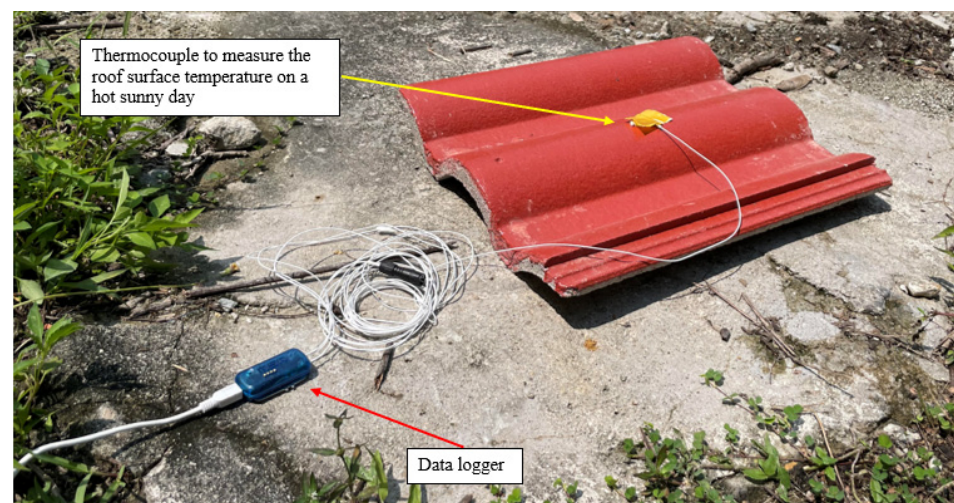


Figure 4. Measurement of the surface temperature of a concrete roof tile in the afternoon of a clear and sunny day.

Figure 5 shows the surface temperature of a concrete roof tile measured on a clear and sunny afternoon in Malaysia. It can be seen that the concrete roof tile surface achieves a constant peak surface temperature of 57–61 °C during the hottest time of the day. The halogen lamps' wattage of the indoor solar simulator is adjusted using a computerized dimmer controller until the concrete roof tile surface achieves a stable temperature of 57–61 °C, similar to the surface temperature achieved by the outdoor measurement.

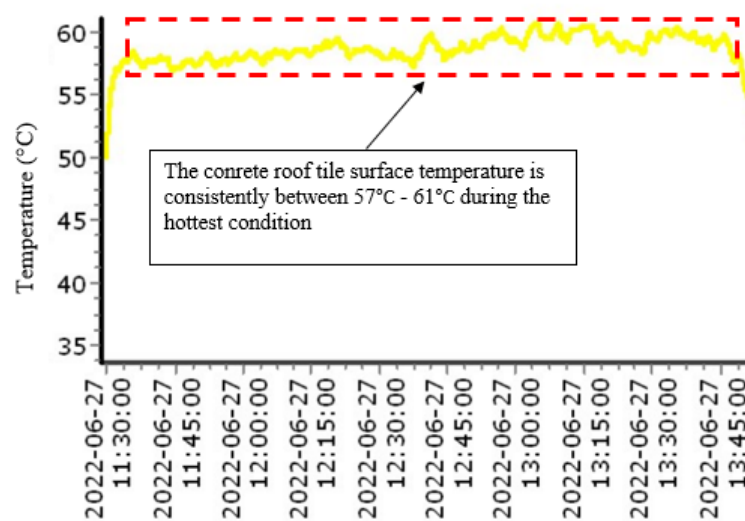


Figure 5. The temperature of the exterior surface of a concrete roof tile during the afternoon of a sunny and clear day.

3.2. Method of Data Collection

Once the halogen lamps are powered up, the Arduino data acquisition system will constantly record and store the readings from the thermocouples and heat flux sensors. As shown in Figure 6, it takes about 4 h for the readings to reach a steady state condition. Once steady state measurements are achieved, the test proceeds for another 3 h to ensure that constant and reliable data are collected. The total time of measurement is 7 h. The steady state values of the surface temperatures and heat flux transmissions are retrieved to compute the RSI value. Each reading was taken three times to ensure the measurements were accurate and reliable.

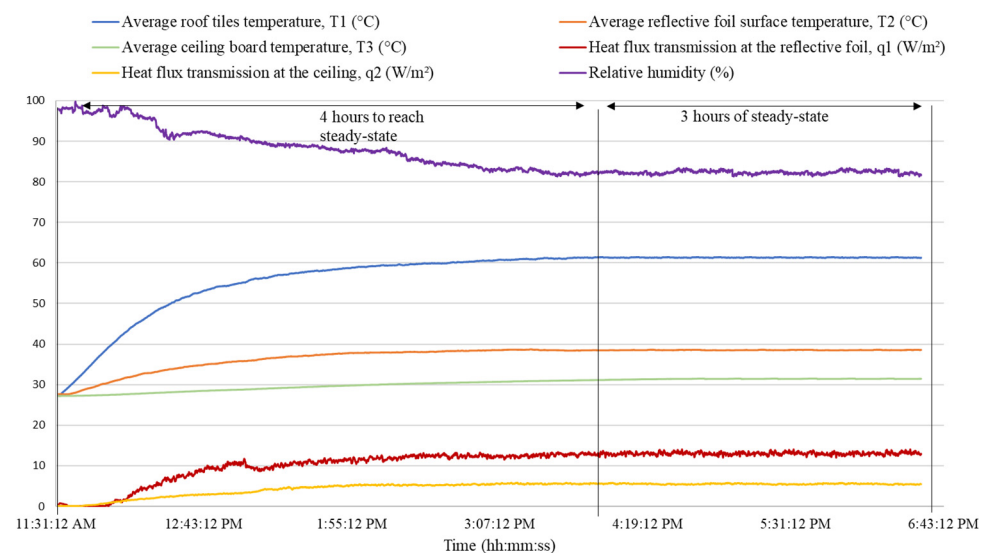


Figure 6. An example of the data retrieved shows the temperature of various roof surfaces, the heat flux transmissions, and the relative humidity inside the laboratory.

Since the test was carried out in a controlled laboratory environment, the relative humidity does not vary significantly between tests. As shown in Figure 6, the relative humidity inside the laboratory reaches a steady state at 82%, which is common in hot and humid climates.

3.3. Method of RSI Value Calculation

The RSI value was calculated using the average method formula detailed in ISO 9869-1:2014 [32]. The total RSI value of the entire roof assembly is the summation of the thermal resistance of the reflective air space, RSI_A , and the thermal resistance of the attic space, RSI_B .

$$RSI_{Total} = RSI_A + RSI_B \quad (1)$$

$$RSI_A = \frac{T_{1_avg} - T_{2_avg}}{q_1} \quad (2)$$

$$RSI_B = \frac{T_{2_avg} - T_{3_avg}}{q_2} \quad (3)$$

where

RSI_A is the RSI value of the reflective air space, m^2K/W ;

RSI_B is the RSI value of the attic air space, m^2K/W ;

RSI_{Total} is the RSI of the entire roof assembly, m^2K/W ;

T_{1_avg} is the average surface temperature of roof tiles, K;

T_{2_avg} is the average surface temperature of reflective foil, K;

T_{3_avg} is the average surface temperature of the ceiling, K;

q_1 is the heat flux transmission at the reflective air space, W/m^2 ;

q_2 is the heat flux transmission at the ceiling, W/m^2 .

3.4. The Residential Roof Configurations Investigated in This Study

Table 3 details the illustrations and compositions of the roof residential configurations studied in this research. The roof configurations chosen for study in this research are commonly found types of roof assemblies for residential buildings in Malaysia. Figures 7 and 8 show the actual assembly of the investigated roof configurations on the indoor solar simulator.

Table 3. The visual representation and composition of the residential roof configurations.

Roof Configuration	Visual Representation	Composition
A0		<ol style="list-style-type: none"> Concrete roof tiles; Attic space; Gypsum ceiling board (thickness 12 mm).
A1		<ol style="list-style-type: none"> Concrete roof tiles; Enclosed air space of 25 mm; Radiant barrier (thickness 0.17 mm); Attic space; Gypsum ceiling board (thickness 12 mm).

Table 3. Cont.

Roof Configuration	Visual Representation	Composition
A2		<ol style="list-style-type: none"> 1. Concrete roof tiles; 2. Enclosed air space of 50 mm; 3. Radiant barrier (thickness 0.17 mm); 4. Attic space; 5. Gypsum ceiling board (thickness 12 mm).
B1		<ol style="list-style-type: none"> 1. Concrete roof tiles; 2. Enclosed air space of 25 mm; 3. Bubble foil reflective insulation (thickness 9 mm); 4. Attic space; 5. Gypsum ceiling board (thickness 12 mm).
B2		<ol style="list-style-type: none"> 1. Concrete roof tiles; 2. Enclosed air space of 50 mm; 3. Bubble foil reflective insulation (thickness 9 mm); 4. Attic space; 5. Gypsum ceiling board (thickness 12 mm).
C1		<ol style="list-style-type: none"> 1. Concrete roof tiles; 2. Mineral glass wool (50 mm); 3. Radiant barrier; 4. Attic space; 5. Gypsum ceiling board (thickness 12 mm).

Table 3. Cont.

Roof Configuration	Visual Representation	Composition
C2		<ol style="list-style-type: none"> 1. Concrete roof tiles; 2. Mineral glass wool (50 mm); 3. Bubble foil reflective insulation (thickness 9 mm); 4. Attic space; 5. Gypsum ceiling board (thickness 12 mm).
D1		<ol style="list-style-type: none"> 1. Concrete roof tiles; 2. Stone wool (50 mm); 3. Radiant barrier (thickness 0.17 mm); 4. Attic space; 5. Gypsum ceiling board (thickness 12 mm).
D2		<ol style="list-style-type: none"> 1. Concrete roof tiles; 2. Stone wool (50 mm); 3. Bubble foil reflective insulation (thickness 9 mm); 4. Attic space; 5. Gypsum ceiling board (thickness 12 mm).



Figure 7. (a) Radiant barrier with battens for roof configuration A1 and A2; (b) bubble foil reflective insulation with battens for roof configuration B1 and B2.



Figure 8. (a) Mineral glass wool (50 mm) on top of the reflective foil with battens for roof configurations C1 and C2; (b) stone wool (50 mm) on top of the reflective foil with battens for roof configurations D1 and D2.

4. Validating the Test Results Obtained from the Indoor Solar Simulator in Relation to the ASHRAE Standard

This section explains the validation of the indoor solar simulator in relation to the RSI values published in the ASHRAE Handbook of Fundamentals Chapter 26, where the RSI values of the enclosed air space adjacent to a surface with low emissivity are listed [33]. The RSI values are based on reducing radiative, convective, and conductive heat transfer in the enclosed air space.

The error bars of the data obtained through the indoor solar simulator are depicted in Figure 9. These bars are found to be within the ASHRAE Standard error margin, which signifies that the error is minimal and thus deemed acceptable. Errors from the measured values are expected because the values in the ASHRAE Standard abided by several simplified assumptions for ideal conditions, such as assuming that the enclosed air space is entirely airtight and unventilated and ignoring any heat transfer from the metal fasteners inside the system [34]. These ideal conditions are challenging to replicate in an empirical condition, which causes errors between the experimental measurement via indoor solar simulator and the ASHRAE Standard. The validation of the novel indoor solar simulator in relation to the ASHRAE standard has been published and can be seen in previous research [35].

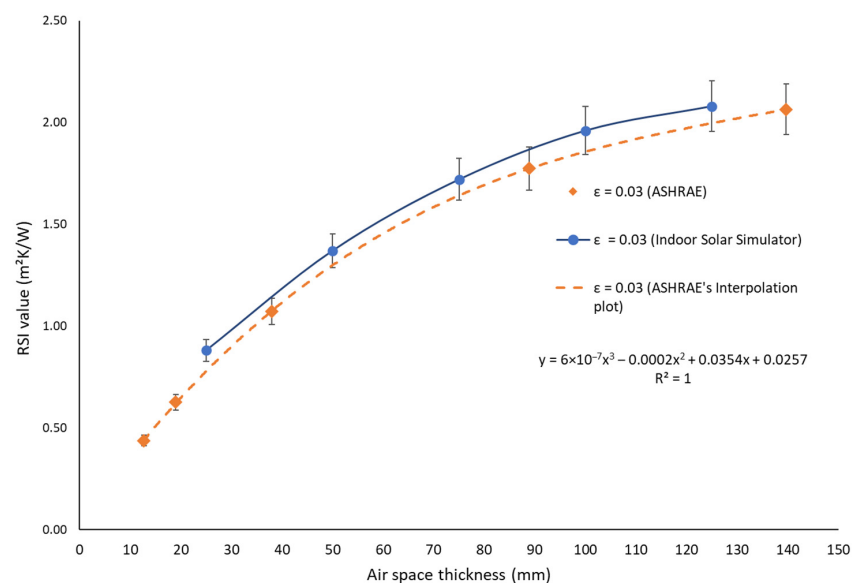


Figure 9. The comparison between the RSI values of various thicknesses of enclosed air space acquired from the indoor solar simulator and ASHRAE Standard [35].

5. Result and Discussion

This section presents the roof tiles-to-ceiling temperature reduction, heat flux transmission at the reflective foil, heat flux transmission at the ceiling, and the total RSI values of every roof configuration tested in this study. The section also evaluates the thermal roof performance achieved by the radiant barrier, mineral glass wool, stone wool, and bubble foil reflective insulation. The section additionally provides an analysis of the impact that changing the thickness of the enclosed air space has on the thermal performance of the roof, as well as the consequences of substituting mass insulation with an enclosed air space.

5.1. The Roof Tiles-to-Ceiling Temperature Reduction, T_1-T_3

Figure 10 shows the roof tiles-to-ceiling temperature reduction for all roof configurations. It can be seen that the pairing of bubble foil reflective insulation with mineral glass wool and stone wool (D1 and D2) has the highest temperature reduction, followed by the pairing of radiant barrier with mineral glass wool and stone wool (C1 and C2). This shows that the low thermal conductivity of mineral glass wool and stone wool can retard high amounts of heat transmission and produce high roof tiles-to-ceiling temperature reduction. The temperature reduction achieved through stone wool is always slightly higher than that of mineral glass wool when combined with a radiant barrier or bubble foil reflective insulation by 1.62% to 2.50%, as seen in Table 4. This is because stone wool has lower thermal conductivity than mineral glass wool. Furthermore, the roof tiles-to-ceiling temperature reduction achieved by the radiant barrier is always lower than the bubble foil reflective insulation by 3.06–6.48%, as seen in Table 5.

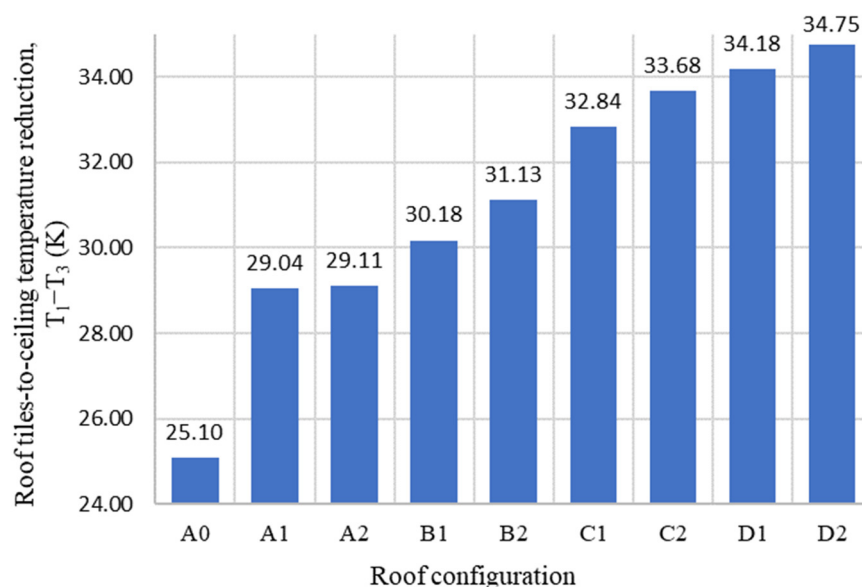


Figure 10. The roof tiles-to-ceiling temperature reduction in the investigated roof assemblies.

Table 4. The percentage difference in roof tiles-to-ceiling temperature reduction between mineral glass wool and stone wool.

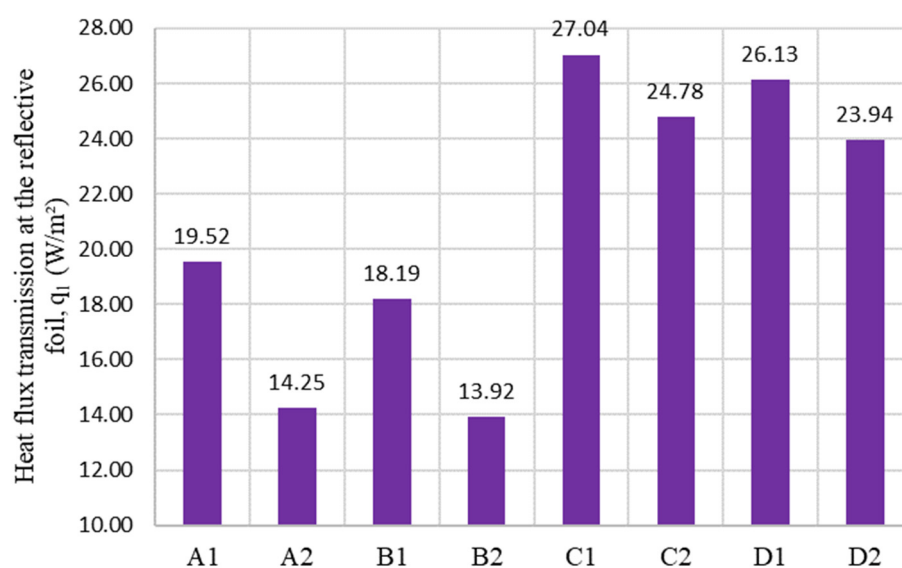
Roof Tiles-To-Ceiling Temperature Reduction, T_1-T_3 (K)			
Type of Reflective Foil	Mineral Glass Wool	Stone Wool	Percentage Difference (%)
Radiant barrier	32.84	33.68	2.50
Bubble foil reflective insulation	34.18	34.75	1.62

Table 5. The percentage difference in the reduction in roof tiles-to-ceiling temperature when comparing radiant barrier and bubble foil reflective insulation.

Roof Tiles-To-Ceiling Temperature Reduction, T_1 – T_3 (K)			
Enclosed Air Space Thickness or Insulation Type	Radiant Barrier	Bubble Foil Reflective Insulation	Percentage Difference (%)
25 mm air space	29.04	30.18	3.76%
50 mm air space	29.11	31.13	6.48%
Mineral glass wool	32.84	34.18	3.93%
Stone wool	33.68	34.75	3.06%

5.2. The Heat Flux Transmission at the Reflective Foil and the Ceiling, q_1 and q_2

Figure 11 shows the heat flux transmission at the reflective foil of all roof configurations. It clearly shows that the combination of reflective foil and mass insulation (C1, C2, D1, and D2) has higher heat flux transmission at the reflective foil than the combination of reflective foil with an enclosed air space (A1, A2, B1, and B2). This is because replacing the enclosed air space with mineral glass wool or stone wool induces higher conductive heat transfer and thus increases the heat flux transmission at the reflective foil. The lowest heat flux transmission at the reflective foil was achieved by bubble foil reflective insulation with a 50 mm enclosed air space (B2), followed by a radiant barrier with a 50 mm enclosed air space (A2), bubble foil reflective insulation with 25 mm enclosed air space (B1), and radiant barrier with 25 mm enclosed air space (A1). This highlights the significance of installing the reflective foil parallel to an enclosed air space to reflect the heat at the reflective foil effectively.

**Figure 11.** The heat flux transmission at the reflective foil of the investigated roof assemblies.

By increasing the thickness of the enclosed air space from 25 mm to 50 mm, the heat flux transmission at the reflective foil is reduced by 27.02% for the radiant barrier and 23.49% for bubble foil reflective insulation, as detailed in Table 6. The bubble foil reflective insulation has lower heat flux transmission at the reflective foil by 2.34–6.84% than the radiant barrier, as seen in Table 7. A higher percentage difference was observed between the radiant barrier and bubble foil reflective insulation at an enclosed air space of 25 mm than at 50 mm. This is because the bubble pockets on the bubble foil reflective insulation become the dominant factor in disrupting the conductive heat transfer in smaller enclosed air spaces. At the 50 mm enclosed air space, the influence of the bubble pockets in reducing the heat gain minimizes as the influence of a thicker enclosed air space becomes more

influential than the bubble pockets. Furthermore, replacing the 50 mm enclosed air space with mass insulation induces the heat flux transmission at the reflective foil by 41.9% and 47.3%, depending on the roof configuration, as seen in Table 8.

Table 6. The percentage difference of 25 mm enclosed air space and 50 mm enclosed air space for radiant barrier and bubble foil reflective insulation.

Heat Flux Transmission at the Reflective Foil, q_1 (W/m ²)			
Type of Reflective Foil	25 mm Enclosed Air Space	50 mm Enclosed Air Space	Percentage Difference (%)
Radiant barrier	19.52	14.25	27.02
Bubble foil reflective insulation	18.19	13.92	23.49

Table 7. The percentage difference of heat flux transmission at between the reflective foil of radiant barrier and bubble foil reflective insulation.

Heat Flux Transmission at the Reflective Foil, q_1 (W/m ²)			
Enclosed Air Space Thickness or Insulation Type	Radiant Barrier	Bubble Foil Reflective Insulation	Percentage Difference (%)
25 mm air space	19.52	18.19	6.84
50 mm air space	14.25	13.92	2.34
Mineral glass wool	27.04	26.13	3.35
Stone wool	24.78	23.94	3.38

Table 8. The comparison of the heat flux transmission at the reflective foil between 50 mm enclosed air space, mineral glass wool, and stone wool.

Heat Flux Transmission at the Reflective Foil, q_1 (W/m ²)			
Type of Reflective Foil	50 mm Air Space	Mineral Glass Wool (50 mm)	Stone Wool (50 mm)
Radiant barrier	14.25	27.04 (↑ 47.3%)	24.78 (↑ 42.5%)
Bubble foil reflective insulation	13.92	26.13 (↑ 46.7%)	23.94 (↑ 41.9%)

Note: ↑ indicates percentage increment of heat flux transmission by mineral glass wool and stone wool compared to 50 mm air space.

Figure 12 shows the roof configuration's heat flux transmission at the ceiling. The least heat flux transmission at the ceiling was achieved by bubble foil reflective insulation with a 50 mm enclosed air space (B2), followed by bubble foil reflective insulation with a 25 mm enclosed air space (B1), bubble foil reflective insulation with stone wool (D2), and bubble foil reflective insulation with mineral glass wool (D1). Figure 12 shows that the bubble foil reflective insulation plays a vital role in minimizing the heat flux transmission at the ceiling. It performs superior radiant barrier by 27.83–43.15% depending on the roof configuration, as detailed in Table 9.

Table 9. The percentage difference of heat flux transmission at the ceiling between the radiant barrier and reflective insulation.

Heat Flux Transmission at the Ceiling, q_2 (W/m ²)			
Enclosed Air Space Thickness or Insulation Type	Radiant Barrier	Bubble Foil Reflective Insulation	Percentage Difference (%)
25 mm air space	9.25	5.26	43.15
50 mm air space	7.27	5.25	27.83
Mineral glass wool	8.87	5.61	36.76
Stone wool	8.72	5.51	36.85

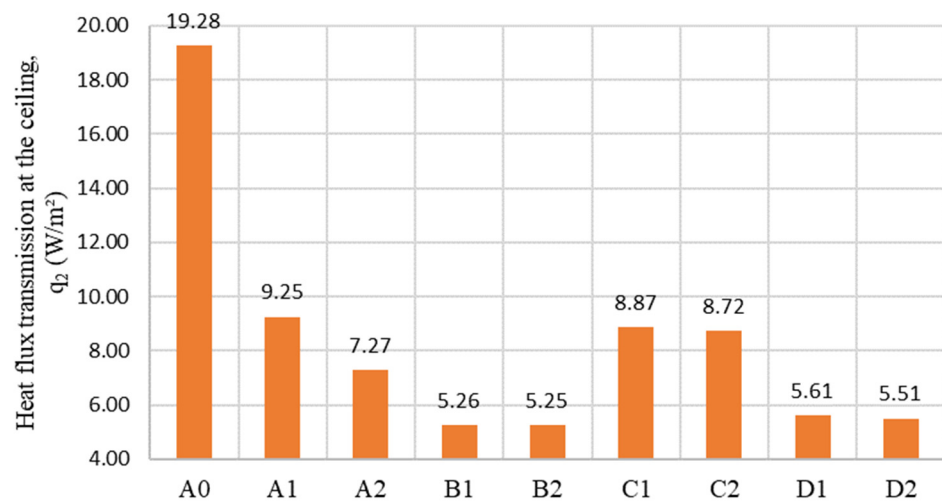


Figure 12. The heat flux transmission at the ceiling of the investigated roof assemblies.

5.3. The Total Thermal Resistance of All Roof Configurations, RSI_{Total}

Figure 13 shows the total RSI values of all roof assemblies investigated in this study. The highest total RSI value was achieved by bubble foil reflective insulation with a 50 mm enclosed air space (B2), followed by bubble foil reflective insulation with a 25 mm enclosed air space (B1), bubble foil reflective insulation with stone wool (D2), bubble foil reflective insulation with mineral glass wool (D1), and radiant barrier with 50 mm air space (A2). These five roof configurations passed the minimum RSI value of 2.5 m²K/W for a lightweight roof, as required in UBBL 38 (A). Figure 13 shows the strong influence of bubble foil reflective insulation in enhancing the thermal performance of a residential type of roof assembly, mainly due to the reduction in heat flux transmission in the attic space, as observed in Figure 12. All four roof configurations which use bubble foil reflective insulation (B1, B2, D1, and D2) passed the minimum RSI of 2.5 m²K/W. Furthermore, the results highlighted the significance of installing the reflective foil parallel to an enclosed air space, as B1 and B2 achieved the two highest RSI values. This observation is also seen in roof configuration A2, which shows that the radiant barrier with a 50 mm enclosed air space can pass the minimum RSI value of 2.5 m²K/W without mineral glass wool or stone wool.

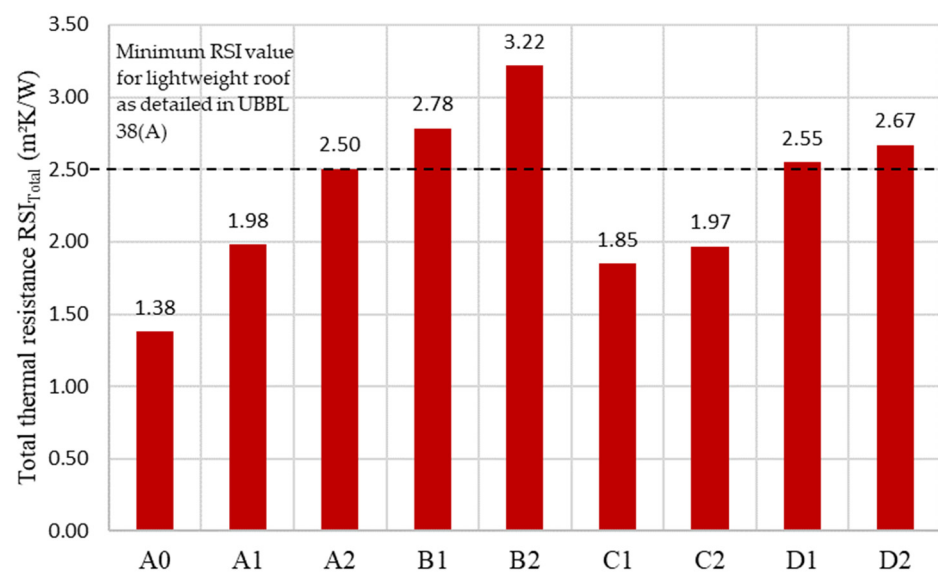


Figure 13. The total RSI values of all roof assemblies.

6. Conclusions

The experimental investigation of the thermal roof performance of residential roofs in Malaysia using a novel indoor solar simulator has been detailed in this research. An earlier section of this article provided a comprehensive explanation of the process used to verify the accuracy of the indoor solar simulator by comparing it to the external surface temperature of a concrete roof tile. On a typical afternoon in Malaysia, an outdoor roof tile surface achieves a peak constant surface temperature between 57 °C and 61 °C. In order to achieve a high degree of accuracy in the measurement conducted with the indoor solar simulator, halogen lamp wattage is altered by using a computerised dimmer controller until the concrete roof tiles achieve a peak surface temperature of about 57 °C to 61 °C.

Then, this research was compared several types of thermal insulation, such as a radiant barrier, bubble foil reflective insulation, mineral glass wool, and stone wool. Some of the significant results are:

1. Bubble foil reflective insulation is much more effective than a radiant barrier in enhancing the thermal efficiency of residential roof assemblies. This is because the heat flux transmission at the ceiling is reduced by 27.83–43.15% when bubble foil reflective insulation is used.
2. When evaluating the thickness of an enclosed air space of 25 mm and 50 mm, it can be seen that the enclosed air space of 50 mm outperforms the 25 mm gap in lowering the heat flux transmission at the reflective foil by a range of 23.49% to 27.02%.
3. By adding more insulating material into the enclosed air space, the heat flux transmission at the reflective foil is enhanced. The addition of mineral glass wool and stone wool to the reflective foil results in a 41.9–47.3% increase in heat flux transmission relative to a 50 mm thick enclosed air space. Consequently, the presence of an air space next to the radiant barrier or bubble reflective insulation decreases the amount of heat transmitted through the reflective foil.
4. Regarding total thermal resistance, it can be concluded that roof configurations with bubble foil reflective insulation resulted in high total thermal resistance and passed the minimum RSI value of 2.5 m²K/W under the UBBL 38 (A) requirements. Most of the roof configurations with radiant barriers did not pass UBBL 38 (A), except for that with an enclosed air space of 50 mm (A2). This shows that it is essential to have a thick, enclosed air space parallel to the radiant barrier to reduce heat gain effectively.

Finally, the novel indoor solar simulator enables accurate and efficient testing of steady-state roof thermal performance. The indoor solar simulator, on the other hand, has several constraints. Restricted by the rig's size, the roof assembly that can be tested is limited to 1.5 m wide and 3 m long. In addition, the maximum height of the attic space is no more than 500 mm, and the shape is fixed with the ceiling parallel to the roof tiles. Therefore, gable and hip roof types cannot be assembled and tested using the indoor solar simulator. Finally, the unique indoor solar simulator could provide a more comprehensive means to evaluate the thermal performance of roofs in a shorter period of time. The findings from this research can help building professionals determine the optimum insulation for residential building roofs in Malaysia.

Author Contributions: M.Z.M.A.: methodology, validation, formal analysis, investigation, writing—original draft, visualisation. C.H.L.: conceptualization, resources, writing—Review and editing, supervision, project administration, funding acquisition. All authors have read and agreed to the published version of the manuscript.

Funding: This research was funded by University Kebangsaan Malaysia (UKM) under the grant RS-2022-001.

Data Availability Statement: The data presented in this study are available on request from the corresponding author. The data are not publicly available due to privacy reasons.

Conflicts of Interest: The authors declare no conflict of interest.

References

1. Energy Commission. *Malaysia Energy Statistics Handbook 2020*; Suruhanjaya Tenaga (Energy Commission): Putrajaya, Malaysia, 2020. Available online: https://www.st.gov.my/en/contents/files/download/116/Malaysia_Energy_Statistics_Handbook_20201.pdf (accessed on 15 September 2023).
2. MS 1525:2014; Energy Efficiency and Use of Renewable Energy for Non-Residential Buildings—Code of Practice. Department of Standards Malaysia: Cyberjaya, Malaysia, 2014.
3. Dominguez, A.; Kleissl, J.; Luvall, J.C. Effects of solar photovoltaic panels on roof heat transfer. *Sol. Energy* **2011**, *85*, 2244–2255. [CrossRef]
4. Zhang, Y.; Sun, H.; Long, J.; Zeng, L.; Shen, X. Experimental and Numerical Study on the Insulation Performance of a Photo-Thermal Roof in Hot Summer and Cold Winter Areas. *Buildings* **2022**, *12*, 410. [CrossRef]
5. Zingre, K.T.; Wan, M.P.; Tong, S.; Li, H.; Chang, V.W.C.; Wong, S.K.; Thian Toh, W.B.; Leng Lee, I.Y. Modeling of cool roof heat transfer in tropical climate. *Renew. Energy* **2015**, *75*, 210–223. [CrossRef]
6. Wang, H.; Huang, Y.; Yang, L. Integrated Economic and Environmental Assessment-Based Optimization Design Method of Building Roof Thermal Insulation. *Buildings* **2022**, *12*, 916. [CrossRef]
7. Lee, S.W.; Lim, C.H.; Salleh, E.@.I.B. Reflective thermal insulation systems in building: A review on radiant barrier and reflective insulation. *Renew. Sustain. Energy Rev.* **2016**, *65*, 643–661. [CrossRef]
8. Reflective Insulation Manufacturers Association International (RIMA-I). *Reflective Insulation, Radiant Barriers and Radiation Control Coatings*; RIMA International: Olathe, KS, USA, 2002; Available online: <https://www.rimainternational.org/pdf/handbook.pdf> (accessed on 25 August 2023).
9. Ashhar, M.Z.M.; Haw, L.C. Recent research and development on the use of reflective technology in buildings—A review. *J. Build. Eng.* **2021**, *45*, 103552. [CrossRef]
10. Materials Market. Glasswool vs. Rockwool: What’s the Difference? 2023. Available online: <https://materialsmarket.com/articles/whats-the-difference-between-rock-mineral-wool-and-glass-mineral-wool/> (accessed on 31 May 2023).
11. BUILD. Rock Wool Insulation. 2023. Available online: <https://build.com.au/rock-wool-insulation#:~:text=How%20does%20rock%20wool%20insulation,air%20pocket%20to%20the%20next> (accessed on 31 May 2023).
12. Shrestha, S.; Miller, W.; Desjarlais, A. *Thermal Performance Evaluation of Attic Radiant Barrier Systems Using the Large Scale Climate Simulator (LSCS)*; ASHRAE Trans.; ASHRAE: Peachtree Corners, GA, USA, 2013.
13. Fantucci, S.; Serra, V. Investigating the performance of reflective insulation and low emissivity paints for the energy retrofit of roof attics. *Energy Build.* **2019**, *182*, 300–310. [CrossRef]
14. Ferreira, M.; Corvacho, H. The effect of the use of radiant barriers in building roofs on summer comfort conditions—A case study. *Energy Build.* **2018**, *176*, 163–178. [CrossRef]
15. Michels, C.; Lamberts, R.; Güths, S. Evaluation of heat flux reduction provided by the use of radiant barriers in clay tile roofs. *Energy Build.* **2008**, *40*, 445–451. [CrossRef]
16. Teh, K.S.; Yarbrough, D.W.; Lim, C.H.; Salleh, E. Field evaluation of reflective insulation in south east Asia. *Open Eng.* **2017**, *7*, 352–362. [CrossRef]
17. Medina, M.A. On the performance of radiant barriers in combination with different attic insulation levels. *Energy Build.* **2000**, *33*, 31–40. [CrossRef]
18. D’Orazio, M.; Di Perna, C.; Di Giuseppe, E.; Morodo, M. Thermal performance of an insulated roof with reflective insulation: Field tests under hot climatic conditions. *J. Build. Phys.* **2013**, *36*, 229–246. [CrossRef]
19. Hauser, G.; Kersken, M.; Sinnesbichler, H.; Schade, A. Experimental and numerical investigations for comparing the thermal performance of infrared reflecting insulation and of mineral wool. *Energy Build.* **2013**, *58*, 131–140. [CrossRef]
20. Amer, E.H. Passive options for solar cooling of buildings in arid areas. *Energy* **2006**, *31*, 1332–1344. [CrossRef]
21. Ong, K.S. Temperature reduction in attic and ceiling via insulation of several passive roof designs. *Energy Convers. Manag.* **2011**, *52*, 2405–2411. [CrossRef]
22. Muhieldeen, M.W.; Yang, L.Z.; Lye, L.C.; Adam, N.M. Analysis of optimum thickness of glasswool roof thermal insulation performance. *J. Adv. Res. Fluid Mech. Therm. Sci.* **2020**, *76*, 1–11. [CrossRef]
23. Roels, S.; Deurinck, M. The effect of a reflective underlay on the global thermal behaviour of pitched roofs. *Build. Environ.* **2011**, *46*, 134–143. [CrossRef]
24. RS Components Ltd. Platinum Resistance Thermometer (PRT) Selection Guide. 2020. Available online: <https://docs.rs-online.com/a6bf/0900766b815e5755.pdf> (accessed on 26 December 2023).
25. International Thermal Instrumental Company. Geo Thermal Heat Flux Transducers. 2023. Available online: <https://thermalinstrumentcompany.com/products/geothermalheatfluxtransducers> (accessed on 26 December 2023).
26. Kipp & Zonen. Pyranometers For the Accurate Measurement of Solar Irradiance. 2023. Available online: <https://www.kippzonen.com/Download/70/Brochure-Pyranometers> (accessed on 26 December 2023).
27. Lama. Lama Roman Tiles. 2014. Available online: <http://lamatiles.com.my/UserFile/editor/file/catalogue-lama-ROMAN-tile-new> (accessed on 15 September 2023).
28. ROCKWOOL. Cool ‘n’ Comfort Blanket and Slab. Available online: <https://p-cdn.rockwool.com/siteassets/rw-sa/product-documentation/product/building-insulation/data-sheets/cool-n-comfort/cool-n-comfort-data-sheet-v2.pdf?f=20210304074052> (accessed on 21 September 2023).

29. Polyglass Fibre Insulation. *Ecowool Brownie Blanket*; Polyglass Fibre Insulation: Perai, Malaysia, 2019.
30. YH Laminated Products Sdn Bhd. SN3-Class-O-Catalog. 2020. Available online: <https://www.yhlp.com.my/wp-content/uploads/2020/05/SN3-Class-O-catalog.pdf> (accessed on 21 September 2023).
31. YH Laminated Products Sdn Bhd. SB400-FR-Catalog. 2020. Available online: <https://www.yhlp.com.my/wp-content/uploads/2020/05/SB400-FR-catalog.pdf> (accessed on 21 September 2023).
32. Kosmina, L. Guide to In-Situ U-Value Measurement of Walls in Existing Dwellings In-Situ Measurement of U-Value ISO 9869. 2016. Available online: www.bre.co.uk/uvalues (accessed on 21 September 2023).
33. ASHRAE. Chapter 26: Heat, air and moisture control in building assemblies—Material properties. In *ASHRAE Handbook of Fundamentals*; ASHRAE: Peachtree Corners, GA, USA, 2009; pp. 26.1–26.22.
34. Pourghorban, A.; Kari, B.M. Evaluation of reflective insulation systems in wall application by guarded hot box apparatus, and comparative investigation with ASHRAE and ISO 15099. *Constr. Build. Mater.* **2019**, *207*, 84–97. [[CrossRef](#)]
35. Ashhar, M.Z.M.; Lim, C.H. Development of an indoor solar simulator for the evaluation of the thermal roof performance for commercial buildings in Malaysia. *J. Build. Eng.* **2023**, *76*, 107204. [[CrossRef](#)]

Disclaimer/Publisher’s Note: The statements, opinions and data contained in all publications are solely those of the individual author(s) and contributor(s) and not of MDPI and/or the editor(s). MDPI and/or the editor(s) disclaim responsibility for any injury to people or property resulting from any ideas, methods, instructions or products referred to in the content.